2,5-Diphenyl-3,4-bis(2-pyridyl)cyclopenta-2,4-dien-1-one as a Redox-Active Chelating Ligand

Ulrich Siemeling,*[a] Imke Scheppelmann,[a] Jürgen Heinze,[b] Beate Neumann,[c] Anja Stammler,[c] and Hans-Georg Stammler[c]

Abstract: 2,5-Diphenyl-3,4-bis(2-pyridyl)cyclopenta-2,4-dien-1-one (**1**), a close relative of tetraphenylcyclopentadienone, is a new ligand platform for use in redox switches and sensors. Compound **1** acts as a molecular electrochemical sensor towards a range of divalent metal ions and exhibits favourable two-wave behaviour. It forms chelates of the type $[(\mathbf{1})MX_2]$, whose stability is enhanced by five orders of magnitude upon one-electron reduction. The bite angle of **1** is close to 90° in these complexes. The attachment of the 14-valence-electron Cp*Co fragment to the cyclopentadienone π system reduces the bite angle and thus modulates the binding characteristics of **1**.

Keywords: chelates · electrochemistry · N ligands · redox switches · UV/Vis spectroscopy

Introduction

Redox-active ligands are of great current interest.[1] They can be used inter alia as molecular electrochemical sensors for the detection of metal cations.[2] The vast majority of such systems contain a redox-active group whose oxidation leads to thermodynamic destabilisation of the metal complex due to electrostatic interactions. Among such ligands, ferrocene derivatives play a prominent role.[3] Ligands which can be reduced are less common, most of them being derived from quinone.[2] For electrostatic reasons, ligand reduction generally leads to a thermodynamic stabilisation of metal complexes, and particularly large enhancements of complex-formation constants of up to about 10^6 have been reported for selected quinone-based systems.[4] In this context we have investigated 2,5-diphenyl-3,4-bis(2-pyridyl)cyclopenta-2,4-dien-1-one (**1**).[5] This compound is a close relative of tetraphenylcyclopentadienone, which exhibits a redox-active cyclopentadienone core that can be reduced reversibly to the corresponding radical monoanion.[6] The coordination chemistry of **1** was completely unexplored prior to our work. Compound **1** combines two well-known ligand platforms, namely, oligopyridine and cylopentadienone. A priori, it may therefore act as a bidentate N,N ligand in Werner-type coordination chemistry and/or as an η^4 ligand in organometallic chemistry. Among such η^4-cyclopentadienone complexes, those containing a cyclopentadienylcobalt(I) fragment are known to show reversible electrochemical behaviour.[6] Therefore, we envisaged that both **1** and its cyclopentadienylcobalt(I) complexes could be used as molecular electrochemical sensors for metals coordinating to the pyridyl nitrogen atoms.

[a] Prof. U. Siemeling, Dr. I. Scheppelmann
Science Department and Center for Interdisciplinary Nanostructure Science and Technology (CINSaT)
University of Kassel
34109 Kassel (Germany)
Fax: (+49) 561-804-4777
E-mail: siemeling@uni-kassel.de

[b] Prof. J. Heinze
Department of Chemistry, University of Freiburg
79104 Freiburg (Germany)

[c] B. Neumann, A. Stammler, Dr. H.-G. Stammler
Department of Chemistry, University of Bielefeld
33501 Bielefeld (Germany)

Results and Discussion

Synthesis and characterisation of compounds

Organometallic complexes: The reaction of **1** with $[CpCo(CO)_2]$ in refluxing *p*-xylene afforded the cyclopentadienone complex $[CpCo(\eta^4\text{-}\mathbf{1})]$ in 89% yield. Less forcing conditions were required for the reaction of **1** with $[Cp^*Co(C_2H_4)_2]$, which proceeded cleanly and swiftly at 60°C in toluene and furnished $[Cp^*Co(\eta^4\text{-}\mathbf{1})]$ in 85% yield (Scheme 1).

Both compounds precipitated from the reaction mixture as red, air-stable, microcrystalline solids which are soluble in polar solvents such as acetonitrile, ethanol and dichloromethane. Crystals suitable for single-crystal X-ray structure analysis were obtained from chloroform in each case. We also determined the structure of **1** for comparison

 DOI: 10.1002/chem.200400465

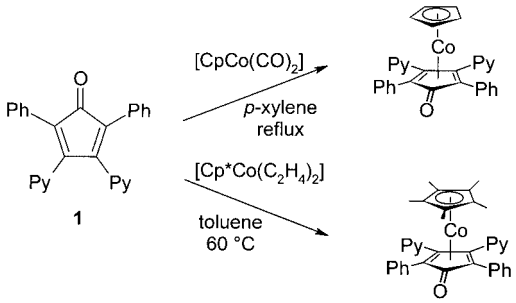

Scheme 1. Synthesis of [CpCo(η^4-**1**)] and [Cp*Co(η^4-**1**)]. Py = 2-pyridyl.

(Figure 1). [CpCo(η^4-**1**)] and [Cp*Co(η^4-**1**)] exhibit sandwich-type structures, and that of the latter is shown in Figure 2.

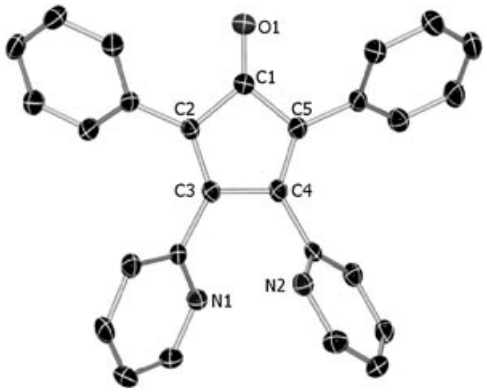

Figure 1. Molecular structure of **1** in the crystal.

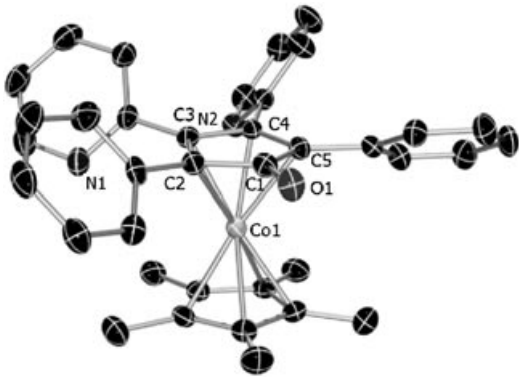

Figure 2. Molecular structure of [Cp*Co(η^4-**1**)] in the crystal.

In each case, the aromatic rings attached to the cyclopentadienone moiety are arranged in an axially chiral paddle-wheel fashion. Both species crystallise as racemic compounds. The aromatic substituents rotate freely on the NMR timescale at room temperature in solution. Metal coordination leads to noticeable changes in the bond parameters of the cyclopentadienone moiety (Table 1), which are typical of such species.[7] The alternating carbon–carbon bond lengths in the diene unit of the five-membered ring of **1** are affected substantially by metal coordination, which results in essentially indistinguishable bond lengths between the four C atoms coordinated to the Co centre in each case. The CO carbon atoms of [CpCo(η^4-**1**)] and [Cp*Co(η^4-**1**)] point away from the metal atom, with folding angles α of the five-membered ring of 12.7 and 7.2°, respectively. This angle has a value of only 1.7° in uncoordinated **1**.

Table 1. Cyclopentadienone fold angle α [°] and selected bond lengths [pm] for ligand **1** and its cyclopentadienylcobalt(I) derivatives.

	1	[Cp*Co(η^4-**1**)]	[CpCo(η^4-**1**)]
C1-C2	151.8(3)	147.7(3)	145.8(7)
C1−C5	151.9(3)	147.6(3)	147.4(6)
C2−C3	134.8(3)	144.3(3)	145.3(7)
C3−C4	152.9(3)	144.2(3)	145.3(6)
C4−C5	135.3(3)	143.6(3)	142.3(7)
C1−O1	120.9(3)	124.7(2)	124.6(6)
α	1.7	7.2	12.7

Delocalisation of electron density from the cyclopentadienylcobalt(I) fragment into the LUMO of **1** leads to a significant elongation of the carbon–oxygen bond of about 4 pm.[7] The weakening of this bond is also consistent with IR spectroscopic data (ν_{CO}: **1** 1715, [CpCo(η^4-**1**)] 1592, [Cp*Co(η^4-**1**)] 1586 cm^{-1}).[8] This transfer of electron density is known to lead to an increase in nucleophilicity of the oxygen atom, which is reflected by reactions with suitable electrophiles to give cobaltocenium species.[7a]

We briefly investigated [Cp*Co(η^4-**1**)] as a representative case in this context, because we were interested to see whether selective reactions at the oxygen atom could be achieved with electrophiles in the presence of the pyridyl N atoms, which act as competing nucleophiles. This indeed proved possible with acetyl chloride, which afforded [Cp*Co(η^5-**1**COMe)]PF_6 as a yellow solid after anion metathesis (Scheme 2). With the softer electrophile methyl triflate (1 equiv), no selective *O*-alkylation was observed, which can be explained in terms of the HSAB principle.[9] Instead, according to NMR spectroscopic results, a mixture of mono-, di- and trimethylated species was obtained together with unconsumed [Cp*Co(η^4-**1**)]. Trimethylation was easily accomplished with an excess of methyl triflate to afford [Cp*Co(η^5-**1**Me_3)]$(CF_3SO_3)_3$ as a yellow solid (Scheme 2). Attempts to remove selectively two methyl

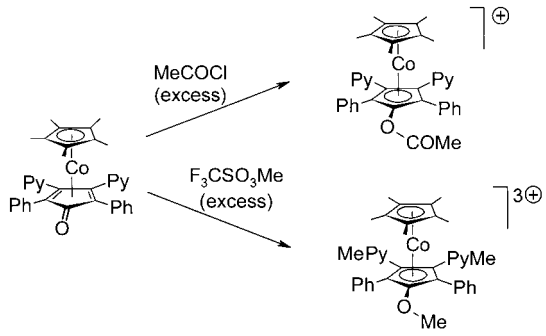

Scheme 2. Acetylation and complete methylation of [Cp*Co(η^4-**1**)]. Py = 2-pyridyl.

groups from this product by reaction with two equivalents of 4-dimethylaminopyridine (DMAP) failed, and a mixture of methylated species again resulted. Attempts were made to achieve selective *O*-alkylation by steric means by utilising trityl chloride as alkylating agent, since trityl chloride in the presence of pyridine is commonly used for the protection of primary alcohols. However, no reaction was observed even after several weeks in dichloromethane solution.

The formation of cobaltocenium species by *O*-acylation or *O*-alkylation is already indicated by the characteristic yellow colour of the respective product and is further supported by NMR spectroscopic data.[10] The ^{13}C NMR signal of the CO carbon atom of [Cp*Co(η^4-**1**)] at 150 ppm experiences a pronounced upfield shift upon acetylation ($\Delta\delta = 36.7$ ppm) or methylation ($\Delta\delta = 22.1$ ppm) of the oxygen atom.

The results of single-crystal X-ray structure analyses, which were performed for [Cp*Co(η^5-**1**COMe)]BPh_4 (Figure 3) and [Cp*Co(η^5-**1**Me_3)]$(CF_3SO_3)_3$ (Figure 4) further corroborate these findings.

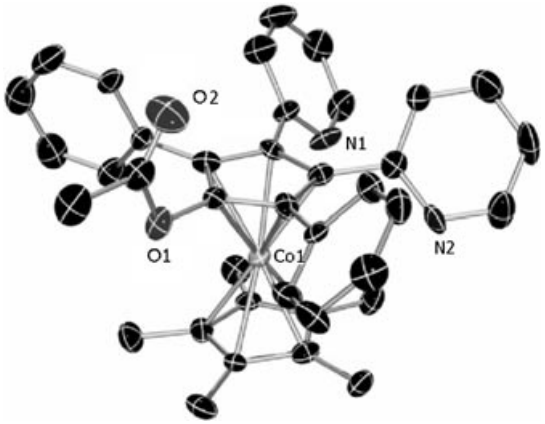

Figure 3. Molecular structure of the cation of [Cp*Co(η^5-**1**COMe)]BPh_4 in the crystal.

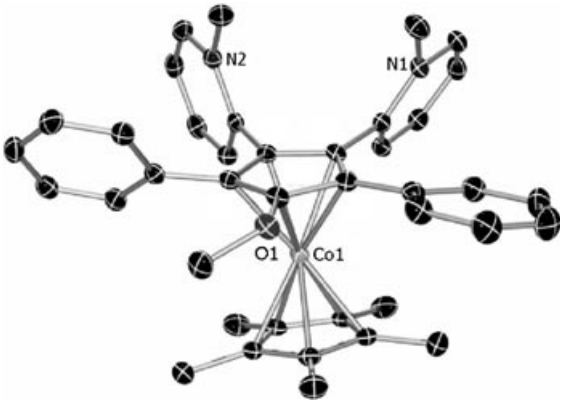

Figure 4. Molecular structure of the cation of [Cp*Co(η^5-**1**Me_3)]$(CF_3SO_3)_3$ in the crystal.

In contrast to the cyclopentadienone complexes [CpCo(η^4-**1**)] and [Cp*Co(η^4-**1**)], the functionalised five-membered rings are essentially planar. Their C–C bond lengths are identical within experimental error and indistinguishable from those within the Cp* ring. The carbon–oxygen bond elongates considerably from 124.7(2) to 140.6(9) and 133.9(2) pm upon acylation and methylation, respectively. In contrast to [CpCo(η^4-**1**)], [Cp*Co(η^4-**1**)] and [Cp*Co(η^5-**1**COMe)]$^+$, which show regular sandwich-type structures with essentially coplanar coordinated π decks, [Cp*Co(η^5-**1**Me_3)]$^{3+}$ exhibits a slightly bent structure with cobalt–carbon bond lengths ranging from 206.02(17) to 212.46(17) pm and a ring tilt angle of 9.2°.

Werner-type complexes: The reaction of **1** with metal dihalides MX_2 in hot ethanol afforded chelate complexes of the type [(**1**)MX_2] ($MX_2 = PdCl_2$, $PtCl_2$, $ZnCl_2$, $HgCl_2$, $HgBr_2$). With the exception of the palladium species, the structures of all these complexes were determined by single-crystal X-ray diffraction. The metal atom is tetracoordinate in each case. The coordination environment is square-planar for d^8-configurated Pt and therefore presumably also for Pd, whereas it is distorted tetrahedral for the other three compounds, in which M is d^{10}-configurated. As a representative example, the structure of the zinc complex is shown in Figure 5. $ZnCl_2$ coordination has no noticeable effect on the

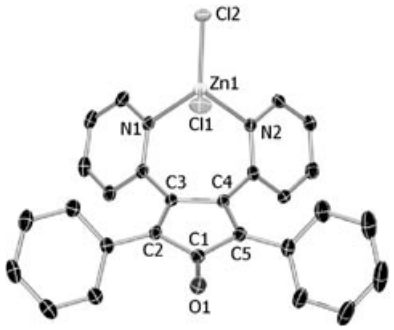

Figure 5. Molecular structure of [(**1**)$ZnCl_2$] in the crystal.

bond lengths of **1**, and the same holds true for the other MX_2 complexes. The seven-membered chelate ring has bond angles at C3 and C4 which deviate only slightly from the corresponding angles in the uncoordinated ligand; the average values are 121° for **1** and 127° for the zinc complex. This effect is even smaller for the other MX_2 complexes. With $CdCl_2$ the chloro-bridged dimer [{(**1**)Cd(μ-Cl)Cl}$_2$] was obtained, which contains two pentacoordinate Cd atoms (Figure 6). Their coordination is best described as distorted square-pyramidal. The Cd–Cl(apical) vectors deviate from the ideal pyramidal orientation by about 8°. The Cd–Cl(apical) distances are 241.29(8) and 240.42(8) pm. These are considerably shorter than the corresponding distances of the bridging basal Cl atoms, which range from 256.33(8) to 259.81(7) pm.

It is instructive to compare the structures of [(**1**)MX_2] with those of unchelated analogues of the type [(py)$_2MX_2$] (py = pyridine). For $MX_2 = ZnCl_2$, the two structures are similar, with pseudotetrahedral zinc coordination. However, the N-Zn-N angle is 106.3(2)° in the unchelated complex,[11] whereas it is only 95.42(5)° in the chelate [(**1**)$ZnCl_2$]. This is

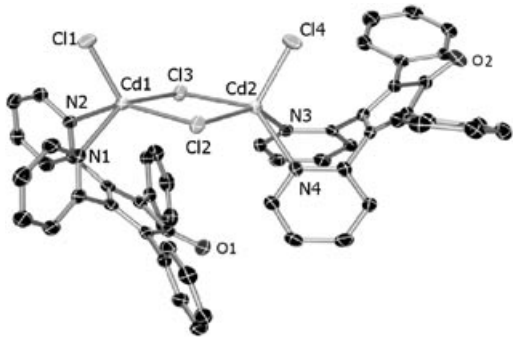

Figure 6. Molecular structure of $[(\mathbf{1})Cd(\mu\text{-}Cl)Cl]_2$ in the crystal.

due to the rigid ligand framework of **1**. In the two mercury compounds, the N-M-N angle is even smaller, namely, 78.30(10)° for $[(\mathbf{1})HgCl_2]$ and 79.08(12)° for $[(\mathbf{1})HgBr_2]$, which is due to the larger size of the coordinated metal atom, which leads to much longer M–N bonds (ca. 206 pm for M = Zn versus ca. 241 pm for M = Hg). The same holds for the cadmium complex, the Cd–N bonds of which range from 232.8(2) to 236.4(2) pm, which results in N-Cd-N angles of 79.85(8) and 77.12(8)°. The pronounced ligand-induced decrease in the N-Zn-N angle does not lead to a concomitant increase of the Cl-Zn-Cl angle, which is 122.172(17)° in the chelate and 120.9(1)° in $[(py)_2ZnCl_2]$,[11] in which repulsive interactions between the two chlorine atoms prevent a closer approach.

Cadmium and mercury have considerably larger ionic radii than zinc, and this allows higher coordination numbers for analogous complexes. Thus, the pyridine complexes for $M = CdCl_2$[12] and $HgCl_2$[13] are coordination polymers of the type $[(py)_2M(\mu\text{-}Cl)_2]_\infty$, which contain infinite chains composed of hexacoordinate chloro-bridged metal atoms bearing two pyridine ligands in *trans* orientation. The architecture of the chelate ligand **1** is incompatible with such a linear N-M-N arrangement and results in a different structure type for cadmium and mercury. We note that the Hg–Cl bond lengths of $[(\mathbf{1})HgCl_2]$ are significantly smaller than the Cd–Cl(apical) distances (ca. 236 versus ca. 241 pm) in $[(\mathbf{1})Cd(\mu\text{-}Cl)Cl]_2$, although the ionic radius of tetracoordinate Hg^{II} is slightly larger than that of pentacoordinate Cd^{II} (110 vs 109 pm). In contrast, the corresponding M–N bond lengths (vide supra) follow the trend of the ionic radii. Just the opposite behaviour has been reported for the polymeric pyridine complexes of $CdCl_2$ and $HgCl_2$ and has been interpreted in terms of a higher degree of metal–nitrogen π backbonding in the case of mercury.

In contrast to its cadmium analogue $[(py)_2Cd(\mu\text{-}Br)_2]_\infty$ and its chloro analogue $[(py)_2Hg(\mu\text{-}Cl)_2]_\infty$, $[(py)_2HgBr_2]$ is monomeric[13] and contains tetracoordinate mercury, the bonding parameters of which are similar to those of $[(\mathbf{1})HgBr_2]$. The Hg–N and Hg–Br bond lengths are about 239 and 248 pm, respectively, for $[(py)_2HgBr_2]$ and about 241 and 249 pm, respectively, for $[(\mathbf{1})HgBr_2]$. The N-Hg-N angle is 90.7(7)° in $[(py)_2HgBr_2]$, and 79.08(12)° in $[(\mathbf{1})HgBr_2]$; the Br-Hg-Br angles are 141.2(1)° for the former, and 137.255(17)° for the latter.

The differences in the coordination behaviour of $ZnCl_2$, $CdCl_2$ and HgX_2 towards **1**, which lead to tetracoordinate mononuclear complexes in the case of zinc and mercury, but to a chloro-bridged dimer exhibiting pentacoordination in the case of cadmium, appear counterintuitive, since they show no consistent relation to the relevant ionic radii. Essentially the same behaviour was observed by Lockhart et al. for a bidentate bis(benzimidazole) ligand.[14] In their case, however, the dimeric cadmium complex is trigonal-bipyramidal with strongly asymmetric chloro bridges. The degree of covalency of the M–X bond increases in the order Zn < Cd < Hg and Cl < Br, reflecting relative valence orbital binding energies.[15] The intricate relationship between valence orbital binding energies and structures in compounds of zinc, cadmium and mercury was investigated by Tossell and Vaughan,[16] and our experimental findings are compatible with their analysis.

From the structures of the Group 10 metal complexes described above it is evident that the bite-angle range of **1** lies around 90°, which is ideal for square-planar coordination. In fact, the N-Pt-N angle in $[(\mathbf{1})PtCl_2]$ is 87.40(12)°, and it is accompanied by a Cl-Pt-Cl angle of 93.39(3)°. The Pt bond lengths and angles are almost identical to those observed for *cis*-$[(py)_2PtCl_2]$.[17]

Finally, the capacity of the organometallic complex $[Cp^*Co(\eta^4\text{-}\mathbf{1})]$ to form Werner-type complexes was tested with the metal dihalides mentioned above. These reactions failed in the case of cadmium and mercury. With zinc chloride, however, the dimetallic chelate $[Cp^*Co(\eta^4\text{-}\mathbf{1})ZnCl_2]$ could be obtained. A downfield shift of the signal of the pyridyl α-protons of about 0.6 ppm was observed in the ^1H NMR spectrum upon metal complexation. The zinc atom is coordinated in an *exo* fashion with respect to the Cp*Co fragment (Figure 7). Metal coordination has no significant effects on the bond lengths of $[Cp^*Co(\eta^4\text{-}\mathbf{1})]$. The angles at the pyridyl-bearing C atoms in the seven-membered chelate ring are slightly smaller than the corresponding angles in $[Cp^*Co(\eta^4\text{-}\mathbf{1})]$; the average values are 127° for $[Cp^*Co(\eta^4\text{-}\mathbf{1})]$ and 121° for the zinc complex. We note that for ligand **1** coordination of $ZnCl_2$ has the opposite effect and leads to an increase of these angles from 121 to 127°. This behaviour may be indicative of additional ring strain in the chelate

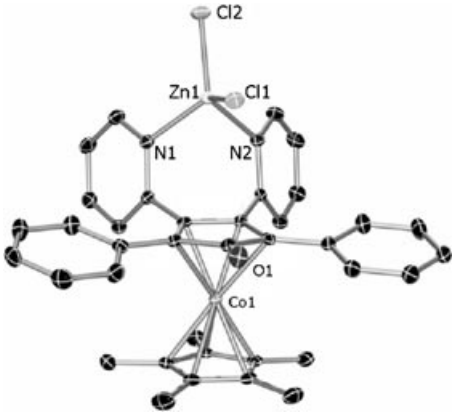

Figure 7. Molecular structure of $[Cp^*Co(\eta^4\text{–}\mathbf{1})ZnCl_2]$ in the crystal.

$[Cp^*Co(\eta^4\text{-}\mathbf{1})ZnCl_2]$ with respect to $[(\mathbf{1})ZnCl_2]$. The bond parameters of the zinc atom of $[Cp^*Co(\eta^4\text{-}\mathbf{1})ZnCl_2]$ are similar to those found for $[(\mathbf{1})ZnCl_2]$; a noticeable difference, however, is the comparatively smaller N-Zn-N (89.34(6) versus 95.42(5)°) and Cl-Zn-Cl angles (113.621(19) versus 122.172(17)°) of the organometallic species. This effect must be due to the presence of the Cp*Co moiety. This unit causes shortening of the bond between the two pyridyl-bearing carbon atoms of about 9 pm in **1** (vide supra) and therefore directly influences the bite angle of the two pyridyl goups attached to these atoms. The bond angles at zinc deviate strongly from those observed for $[(py)_2ZnCl_2]$ (N-Zn-N 106.3(2), Cl-Zn-Cl 120.9(1)°, vide supra) and are indicative of ring strain, which conceivably leads to destabilisation of the complex. In fact, further investigations showed that the complex-formation constant of $[Cp^*Co(\eta^4\text{-}\mathbf{1})ZnCl_2]$ in acetonitrile is lower by one order of magnitude than that of the less strained $[(\mathbf{1})ZnCl_2]$ (vide infra). In the case of cadmium and mercury, the ligand $[Cp^*Co(\eta^4\text{-}\mathbf{1})]$ would cause even more acute bond angles than those observed in the case of **1**, for which chelates of the type $[(\mathbf{1})MX_2]$ exhibit N-M-N angles that are already smaller than 80° for M = Cd and Hg. Obviously, complex formation does not occur under these circumstances.

The ionic radii of square-planar tetracoordinate Pd^{II} (78 pm) and Pt^{II} centres (74 pm) are practically identical with that of tetracoordinate Zn^{II} (74 pm). Thus, complex formation occurred with $PdCl_2$ and $PtCl_2$, as evidenced by ^1H NMR spectroscopic monitoring of the reaction in deuterated methanol. Again, a downfield shift of the signal of the pyridyl α-protons of about 0.6 ppm was observed. The products proved to be only sparingly soluble in common organic solvents and undergo light-induced decomposition with formation of elemental palladium and platinum, respectively. Only $[Cp^*Co(\eta^4\text{-}\mathbf{1})PdCl_2]$ could be obtained in pure form.

The cobaltocenium derivative $[Cp^*Co(\eta^5\text{-}\mathbf{1}COMe)]^+$ proved to be unable to form complexes with the metal dihalides investigated, which is probably due to repulsive electrostatic effects.

Electrochemistry: Cyclic voltammetry revealed that compound **1** is reversibly reduced to its radical anion. The half-wave potential is −1.37 V in CH_2Cl_2 and −1.23 V in CH_3CN (vs ferrocenium/ferrocene).[18] Coordination of a cyclopentadienylcobalt(I) fragment to the π system of **1** leads to a rather dramatic electrochemical effect, which is based on the fact that electron density is delocalised from the organometallic moiety into the LUMO of **1** (vide supra). $[CpCo(\eta^4\text{-}\mathbf{1})]$ and $[Cp^*Co(\eta^4\text{-}\mathbf{1})]$ undergo reversible reduction at −1.89 and −1.97 V, respectively, in acetonitrile; the more electron-rich Cp* derivative is harder to reduce.

The redox behaviour of **1** is also rather sensitive to metal coordination at the pyridyl groups. An investigation of the chelates of type $[(\mathbf{1})MX_2]$ revealed that for M = Hg irreversible reduction occurred at about −0.75 V and led to deposition of elemental mercury on the electrode. The dimeric cadmium complex also showed irreversible behaviour, with a broad reduction peak at about −1.05 V, which may be due to the formation of monomeric fragments. All other complexes showed quasireversible electrochemical behaviour (Table 2).

Table 2. Half-wave potentials [V] (vs ferrocenium/ferrocene) for the reduction processes exhibited by **1** and its zinc, palladium and platinum complexes.

	1	$[(\mathbf{1})ZnCl_2]$	$[(\mathbf{1})PdCl_2]$	$[(\mathbf{1})PtCl_2]$
$E_{1/2}$ (CH_2Cl_2)[a]	−1.37	−1.03	−1.05	−1.00
$\Delta E_{1/2}$[b]		0.34	0.32	0.37
$E_{1/2}$ (CH_3CN)[a]	−1.23	−0.93		
$\Delta E_{1/2}$[b]		0.30		

[a] Scan rate 0.10 V s^{-1}, 0.1 M $[NBu_4]PF_6$ supporting electrolyte, $\Delta E_p \approx$ 0.10 V. [b] Shift of the half-wave potential with respect to that of **1** in the same solvent.

For the sensing of nonpolarisable ions, the shift of the half-wave potential is governed by Coulomb interactions, and therefore large values can be expected only when the ion-binding site is in close proximity to the redox-active unit. This is particularly important for the highly polar solvents generally used for the investigation of ionic species, since there is an inverse dependence of $\Delta E^{0\prime}$ on the dielectric constant of the medium, as is shown by Equation (1) (n: number of electrons transferred during the redox process, F: Faraday constant, N_A: Avogadro constant, Q_{guest}: charge of the guest ion, ΔQ_{sensor}: charge change of the sensor caused by the redox process, ε_0: vacuum permittivity, ε: dielectric constant of the solvent, d: distance between the redox-active centre and the point charge of the guest).

$$nF|\Delta E^{0\prime}| = N_A Q_{guest} \Delta Q_{sensor} / 4\pi\varepsilon_0 \varepsilon d \quad (1)$$

In the present system, the shift of the half-wave potential induced by metal complexation is rather large in each case. As expected, the effect is more pronounced in dichloromethane ($\varepsilon = 8.93$) than in the more polar acetonitrile ($\varepsilon = 36.64$).[19] The $\Delta E_{1/2}$ values are similar for the three complexes, since the metal centres have similar ionic radii (vide supra) and identical ligands.

The metal complexes of the type $[Cp^*Co(\eta^4\text{-}\mathbf{1})MCl_2]$ show irreversible electrochemical behaviour for M = Zn and Pd. In the case of zinc, a reduction wave at $E_p = -1.34$ V is observed. However, the oxidative process leads to a broad wave at about −1.00 V, which is probably due to the formation of elemental zinc. The palladium complex shows irreversible reduction at $E_p = -1.43$ V, whereupon a reversible redox wave at $E_{1/2} = -2.12$ V is observed. This is close to, but not identical with, the redox potential of $[Cp^*Co(\eta^4\text{-}\mathbf{1})]$ (−1.97 V). The nature of the species responsible for this redox wave therefore remains unclear. The purity of the platinum complex $[Cp^*Co(\eta^4\text{-}\mathbf{1})PtCl_2]$, although not satisfactory for analytical purposes, was sufficient for investigations by cyclic voltammetry. A quasireversible reduction at $E_{1/2} = -1.75$ V was observed for this compound. The $\Delta E_{1/2}$ value of 0.22 V with respect to $[Cp^*Co(\eta^4\text{-}\mathbf{1})]$ is smaller than that of 0.37 V observed for **1** and $[(\mathbf{1})PtCl_2]$, even when it is taken into account that the latter value was determined in the less polar solvent dichloromethane.

Determination of complex-formation constants: The redox and coordination equilibria in the square scheme shown in Scheme 3 are the basis for the use of **1** as a molecular electrochemical sensor. We were able to elucidate the thermodynamics involved by a combination of UV/Vis spectroscopic and electrochemical studies.

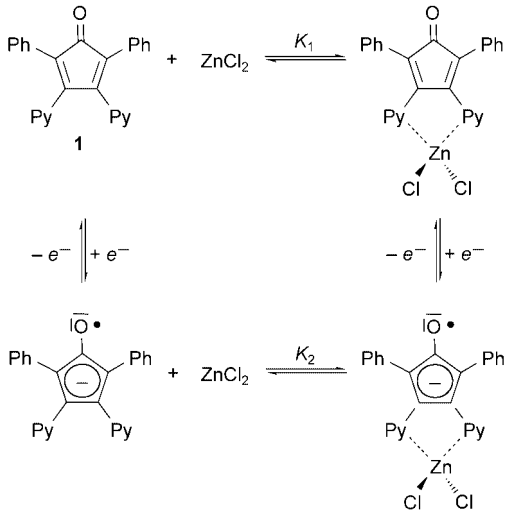

Scheme 3. Scheme for the binding equilibria of **1** and zinc chloride.

A UV/Vis titration experiment was performed with **1** and $ZnCl_2$ in acetonitrile solution (Figure 8). The absorption due to the ligand **1** ($\lambda_{max}=255$ nm) decreases gradually, whereas

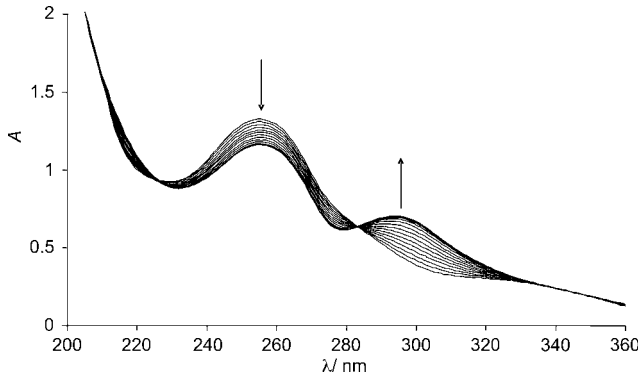

Figure 8. Effect of $ZnCl_2$ on the UV/Vis spectrum of **1** in acetonitrile solution (portionwise addition of 1 equiv).

that of the corresponding zinc complex ($\lambda_{max}=297$ nm) increases gradually upon stepwise addition of zinc chloride. The presence of isosbestic points proves that a simple equilibrium between just two absorbing species is operative here. Monitoring the absorbance at a constant wavelength shows that the zinc containing species is a 1:1 complex (Figure 9), in accord with the crystallographically characterised chelate [(**1**)$ZnCl_2$] (vide supra).

The complex-formation constant K_1 for [(**1**)$ZnCl_2$] can be obtained from the UV/Vis data, provided the extinction coefficients of the two absorbing species are known for a given

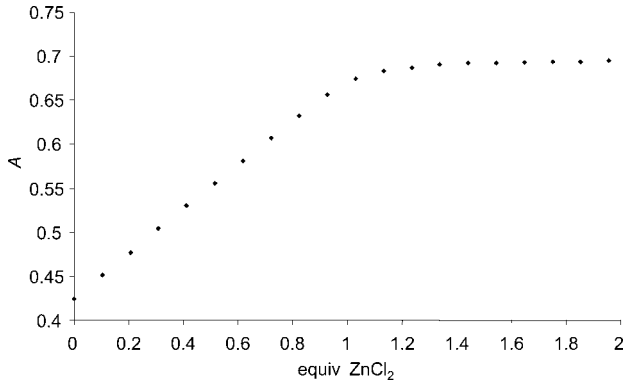

Figure 9. Absorbance at $\lambda=297$ nm during the titration of **1** with zinc chloride (portionwise addition of 2 equiv) in acetonitrile.

wavelength, by using an established procedure (see Experimental Section). In this case, the wavelength of choice is 297 nm, since here the largest changes in absorbance occur during the titration experiment. The extinction coefficient of **1** at $\lambda=297$ nm, as determined at 298 K from UV/Vis spectra of this compound by using the Lambert–Beer law ($A=\varepsilon cd$), is $9130\,M^{-1}cm^{-1}$. The corresponding value for the zinc complex can be approximated from the titration experiment, under the assumption that it is the only absorbing species in the presence of an excess of zinc chloride (see Figure 9). This procedure leads to a value of $14900\,M^{-1}cm^{-1}$. The following fitting procedure affords values of $8997\,M^{-1}cm^{-1}$ and $14927\,M^{-1}cm^{-1}$ for ε_{297} of **1** and [(**1**)$ZnCl_2$], respectively, and yields a value of $(1.9\pm0.2)\cdot10^6\,M^{-1}$ for K_1 at 298 K. This corresponds to a pK_1 value of -6.276 ± 0.046.

The complexation of zinc chloride by **1** in acetonitrile solution was also monitored electrochemically in a titration experiment using square-wave voltammetry (Figure 10).

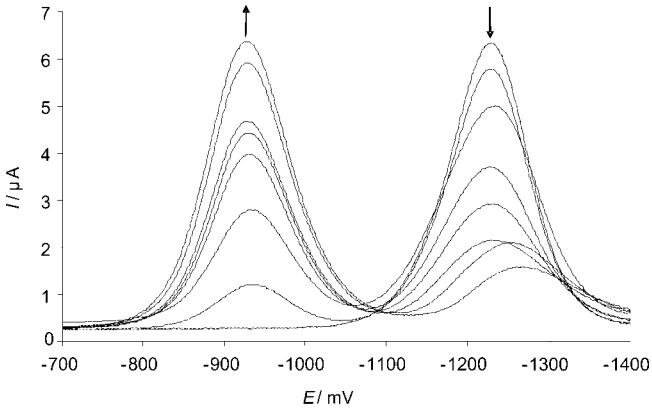

Figure 10. Effect of zinc chloride (portionwise addition of 1 equiv) on the square-wave voltammogram of **1** (acetonitrile, 0.1 M [NBu_4][PF_6]).

Addition of a small amount of $ZnCl_2$ (<10 mol%) leads to the appearance of a new redox wave in the square-wave voltammogram of **1**, cathodically shifted by 0.30 ± 0.01 V, which corresponds to an enormous increase of the metal-binding constant by five orders of magnitude. The two-wave behaviour observed is characteristic for systems showing

very large complex-formation constants, typically on the order of $10^6\,M^{-1}$,[2b] which is nicely compatible with the value of -6.276 ± 0.046 determined for pK_1. The pK_2 value for the reduced species in Scheme 3, as estimated[2b] from K_1 and the electrochemical potential shift of 0.30 ± 0.01 V, is -11.35 ± 0.15 at 298 K.

A UV/Vis titration experiment was also performed for the complexation of zinc chloride by [Cp*Co(η^4-**1**)] in acetonitrile (Figure 11).

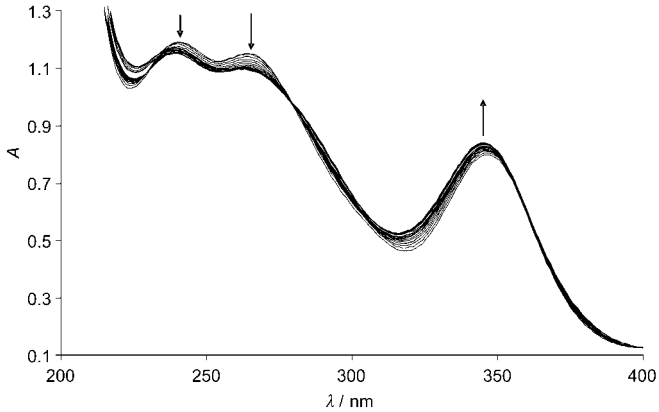

Figure 11. Effect of $ZnCl_2$ on the UV/Vis spectrum of [Cp*Co(η^4–**1**)] in acetonitrile solution (portionwise addition of 1 equiv).

Again, the presence of an isosbestic point shows that a simple equilibrium between just two absorbing species is involved. By a procedure analogous to that described above for [(**1**)$ZnCl_2$], the complex-formation constant of [Cp*Co(η^4-**1**)$ZnCl_2$] in acetonitrile was determined to be $(1.3\pm0.2)\times10^5\,M^{-1}$ at 298 K, with extinction coefficients at $\lambda=266$ nm of 24700 and $23200\,M^{-1}\,cm^{-1}$ for [Cp*Co(η^4-**1**)] and [Cp*Co(η^4-**1**)$ZnCl_2$], respectively. This result shows that the presence of the Cp*Co fragment leads to a pronounced destabilisation of the chelate by approximately one order of magnitude, for which the main reason is the unfavourable change in bite angle induced by the organometallic moiety (vide supra).

Conclusion

We have explored the coordination chemistry of 2,5-diphenyl-3,4-bis(2-pyridyl)cyclopenta-2,4-dien-1-one (**1**). This compound can act as a bidentate ligand that forms stable chelates with a range of metal dihalides. Pseudotetrahedral, square-planar and square-pyramidal coordination has been observed. Compound **1** is a redox-active ligand showing well-behaved electrochemistry. It can therefore exhibit switchable binding. In the case of the zinc complex [(**1**)$ZnCl_2$], enhancement of the complex-formation constant by five orders of magnitude is observed upon one-electron reduction. This is similar to the best results obtained with quinone-based switches. Compound **1** can be used as a molecular electrochemical sensor for the detection of divalent metal ions in solution, since it shows favourable two-wave behaviour. In contrast to quinone-based systems, the binding characteristics of **1** can easily be modulated by attachment of a suitable organometallic fragment to the redox-active moiety. The complex-formation constant of [Cp*Co(η^4-**1**)$ZnCl_2$] is approximately ten times smaller than that of [(**1**)$ZnCl_2$].

Compound **1** is a new and convenient ligand platform for use in redox switches and sensors, since cyclopentadienone derivatives have not been used before in this context. Its versatility as a ligand is enhanced by the fact that its binding characteristics can be influenced through secondary interactions involving coordination of the cyclopentadienone π system. We envisage that fine-tuning of these effects will be possible by using 14-valence-electron complex fragments with different stereoelectronic properties. Furthermore, it is conceivable that attaching other donor sets such as S,S and O,O to the cyclopentadienone ring may give rise to further interesting redox-active ligands. Work with the corresponding 2-thienyl-[20] and 2-furyl-substitued[20,21] analogues of **1** is in progress.

Experimental Section

General: [Cp*Co(C_2H_4)$_2$] was prepared according to a published procedure.[22] All other compounds were commercially available. Synthetic work involving air-sensitive compounds was performed under an atmosphere of dry argon or nitrogen by using standard Schlenk techniques or a conventional glove box. Solvents and reagents were appropriately dried and purified. NMR: Bruker Avance DRX 500 and Varian Unity INOVA 500 (500.13 MHz for ^{1}H); MS: Finnigan MAT 8430 (EI) or PE Biosystems Voyager System 1161 (ESI; MALDI-TOF, 2,5-dihydroxybenzoic acid calibration matrix); IR: Bruker Vector 22 and Mattson Genesis FT-IR; UV/Vis: Perkin Elmer Lambda 40, an absorbance correction taking into account the decreasing analyte concentration during the course of the titration experiments was performed; elemental analyses: Beller (Göttingen), H. Kolbe (Mülheim an der Ruhr) and microanalytical laboratory of the University of Bielefeld.

Determination of complex-formation constants: For the complex-formation equilibrium $L+M\Leftrightarrow LM$ the expression for the equilibrium constant is $K=c_Lc_M/c_{LM}$ (c = equilibrium concentration). When c_L^0 and c_M^0 are the starting concentrations used, the respective equilibrium concentrations are $c_L=c_L^0-c_{LM}$ and $c_M=c_M^0-c_{LM}$. Substituting these into the expression for K gives $K=(c_L^0-c_{LM})(c_M^0-c_{LM})/c_{LM}$. From this quadratic equation it follows that the unknown equilibrium concentration of the complex is $c_{LM}=(c_L^0+c_M^0+K)/2-[(c_L^0+c_M^0+K)^2/4-c_L^0c_M^0]^{0.5}$. The absorbance at a given wavelength λ is described by the Lambert–Beer law: $A/d=\varepsilon c$. In the present system, two absorbing species are present, namely, L and LM. Therefore, $A/d=\varepsilon_Lc_L+\varepsilon_{LM}c_{LM}$. Since $c_L=c_L^0-c_{LM}$, this equation can be written as $A/d=\varepsilon_L(c_L^0-c_{LM})+\varepsilon_{LM}c_{LM}=\varepsilon_Lc_L^0+(\varepsilon_{LM}-\varepsilon_L)c_{LM}$. With $c_{LM}=(c_L^0+c_M^0+K)/2-[(c_L^0+c_M^0+K)^2/4-c_L^0c_M^0]^{0.5}$ this can be written as $A/d=\varepsilon_L(c_L^0-c_{LM})+\varepsilon_{LM}c_{LM}=\varepsilon_Lc_L^0+(\varepsilon_{LM}-\varepsilon_L)\{(c_L^0+c_M^0+K)/2-[(c_L^0+c_M^0+K)^2/4-c_L^0c_M^0]^{0.5}\}$. The complex formation constant K can be obtained from this equation by standard fitting procedures, given that the following values are known in the UV/Vis titration experiment: V_s (sample volume at the start), c_{Ls} (starting concentration of L in the sample), c_{Mt} (concentration of M in the titre solution), v (volume of titre solution added). During the titration, the total volume is $V=V_s+v$. Consequently, the relevant concentrations at any stage of the titration are $c_L^0=c_{Ls}(V_s/V)$ and $c_M^0=c_{Mt}(v/V)$. The experimental determination of ε_L is straightforward, and ε_{LM} can be obtained by extrapolation from the titration experiment, under the assumption that LM is the only absorbing species in the presence of an excess of M.

Electrochemical investigations: Experiments involving [CpCo(η^4-**1**)], [Cp*Co(η^4-**1**)] and complexes of the type [Cp*Co(η^4-**1**)MCl_2] were carried out in specially constructed cells containing an internal drying

column with highly activated alumina. The working electrode was a Pt disc sealed in soft glass (1.0 mm diameter). A Pt wire was used as the counterelectrode. Potentials were calibrated with ferrocene [$E_{1/2}$(ferrocenium/ferrocene) = 0.38 V versus Ag/AgCl/KCl(aq)]. The setup was controlled by a Jaissle potentiostat IMP88. Material and apparatus for all other electrochemical studies have been described elsewhere.[23]

2,5-Diphenyl-3,4-bis(2-pyridyl)cyclopenta-3,4-diol-1-one: The compound was prepared previously,[5] but analytical data were unavailable. Powdered potassium hydroxide (2.00 g, 35.6 mmol) was added to a vigorously stirred solution of dibenzyl ketone (33.3 g, 158 mmol) and 2,2′-pyridil (25.1 g, 119 mmol) in ethanol (400 mL). After 1 h, the voluminous white precipitate was filtered off with suction, washed with ethanol (3 × 30 mL) and dried in vacuo. Yield 47.5 g (94 %). ^{1}H NMR ($CDCl_3$): δ = 4.78 (s, 2H), 6.98 (m, 4H), 7.11 (m, 2H), 7.22 (m, 6H), 7.36 ("d", apparent J = 8.1 Hz, 2H), 7.52 (m, 2H), 8.37 (d, J = 5.0 Hz, 2H), 8.74 ppm (s, 2H); ^{13}C{^{1}H} NMR ($CDCl_3$): δ = 65.9, 82.1, 122.4, 123.2, 127.1, 127.7, 130.9, 133.3, 137.3, 146.5, 162.5, 213.3 ppm; IR (KBr): $\tilde{\nu}$ = 1743 (ν_{CO}) cm^{-1}; MS (EI): m/z: 422 $[M]^+$; elemental analysis (%) calcd for $C_{27}H_{22}N_2O_3$ (422.48): C 76.76, H 5.25, N 6.63; found: C 76.92, H 5.40, N 6.62.

1: The synthesis was performed by using a dehydration protocol developed by Hughes et al. for the synthesis of 1,5-di-*tert*-butyl-1,3-cyclopentadiene,[24] since this gave yields superior to those reported by Eistert et al.[5] $POCl_3$ (15.0 g, 97.8 mmol) was added to a suspension of 2,5-diphenyl-3,4-bis(2-pyridyl)cyclopenta-3,4-diol-1-one (21.1 g, 50.0 mmol) in pyridine (90 mL). The reaction mixture was stirred at 85 °C for 14 h and was subsequently allowed to cool to room temperature. Volatile components were removed in vacuo. The solid residue was dissolved in dichloromethane (500 mL). The solution was cooled to 0 °C and treated with a saturated aqueous solution of sodium carbonate (100 mL). After gas evolution had stopped, the organic layer was separated, washed with water (2 × 100 mL) and dried with sodium sulfate. The solution was reduced to dryness in vacuo and the brownish red crude product recrystallised from ethanol to afford the product as dark red crystals. Yield 14.3 g (74 %). ^{1}H NMR ($CDCl_3$): δ = 7.06 (m, 2H), 7.23 (m, 12H), 7.51 (m, 2H), 8.32 ppm (d, J = 4.4 Hz, 2H); ^{13}C{^{1}H} NMR ($CDCl_3$): δ = 122.3, 125.0, 126.7, 128.0, 128.2, 130.0, 130.2, 135.9, 149.0, 153.1, 153.2, 200.7 ppm; IR (KBr): $\tilde{\nu}$ = 1715 (ν_{CO}) cm^{-1}; MS (EI): m/z: 386 $[\mathbf{1}]^+$; elemental analysis (%) calcd for $C_{27}H_{18}N_2O$ (386.45): C 83.92, H 4.70, N 7.25; found: C 83.93, H 4.74, N 7.23.

[CpCo(η^4-1)]: A solution of **1** (3.86 g, 10.0 mmol) and $[CpCo(CO)_2]$ (1.81 g, 10.1 mmol) in *p*-xylene (20 mL) was heated to reflux for 14 h. The mixture was allowed to cool to room temperature. The dark red, microcrystalline precipitate was isolated by filtration, washed with *n*-hexane (3 × 20 mL) and dried in vacuo. Yield 4.54 g (89 %). ^{1}H NMR ($CDCl_3$): δ = 4.98 (s, 5H), 7.09 ("t", 2H), 7.15 (d, J = 7.7 Hz, 2H), 7.22 (m, 6H), 7.42 ("t", 2H), 7.63 ("d", apparent J = 3.8 Hz, 4H), 8.41 ppm (d, J = 3.4 Hz, 2H); ^{13}C{^{1}H} NMR ($CDCl_3$): δ = 79.1, 85.9, 92.8, 122.1, 126.7, 127.1, 127.8, 128.9, 130.3, 133.1, 135.2, 149.1, 153.6 ppm; IR (KBr): $\tilde{\nu}$ = 1593 (ν_{CO}) cm^{-1}; MS (ESI): m/z: 511 $[M]^+$; elemental analysis (%) calcd for $C_{32}H_{23}N_2CoO$ (510.49): C 75.29, H 4.54, N 5.49; found: C 76.04, H 4.93, N 4.96.

[Cp*Co(η^4-1)]: A solution of **1** (3.86 g, 10.0 mmol) and $[Cp^*Co(C_2H_4)_2]$ (2.50 g, 10.0 mmol) in toluene (100 mL) was heated to 50 °C for 14 h. The mixture was allowed to cool to room temperature. The red, microcrystalline precipitate was isolated by filtration, washed with *n*-hexane (2 × 20 mL) and dried in vacuo. Yield 4.94 g (85 %). ^{1}H NMR ($CDCl_3$): δ = 1.45 (s, 15H), 6.95 (d, J = 7.8 Hz, 2H), 7.05 ("t", 2H), 7.14 (m, 6H), 7.35 ("t", 2H), 7.72 ("d", apparent J = 6.8 Hz, 4H), 8.45 ppm (d, J = 4.3 Hz, 2H); ^{13}C{^{1}H} NMR ($CDCl_3$): δ = 8.0, 77.8, 90.9, 92.6, 121.6, 126.2, 126.3, 127.2, 130.0, 132.6, 135.0, 148.9, 150.0, 154.9 ppm; IR (KBr): $\tilde{\nu}$ = 1562 (ν_{CO}) cm^{-1}; MS (ESI): m/z: 581 $[M]^+$; elemental analysis (%) calcd for $C_{37}H_{33}N_2CoO$ (580.62): C 76.54, H 5.73, N 4.82; found: C 75.98, H 5.72, N 4.77.

[Cp*Co(η^5-1COMe)]PF$_6$: Acetyl chloride (6.0 mL) was added dropwise to [Cp*Co(η^4-**1**)] (181 mg, 0.31 mmol). The resultant yellow solution was stirred for 1 h and subsequently reduced to dryness in vacuo. The remaining light orange solid was dissolved in ethanol (5 mL). The yellow product was precipitated by dropwise addition of a saturated aqueous solution of ammonium hexafluorophosphate, filtered off, washed with diethyl ether (10 mL) and *n*-hexane (10 mL) and dried in vacuo. Yield 234 mg (80 %). ^{1}H NMR ($CDCl_3$): δ = 1.69 (s, 15H), 2.33 (s, 3H), 6.68 (d, J = 7.8 Hz), 7.05 (m, 4H), 7.27 (m, 2H), 7.35 ("t", 4H), 7.42 (m, 2H), 7.53 (m, 2H), 8.51 ppm (d, J = 5.4 Hz); ^{13}C{^{1}H} NMR ($CDCl_3$): δ = 8.9, 20.6, 93.7, 94.1, 99.6, 113.3, 123.9, 125.9, 126.6, 129.1, 129.6, 130.1, 136.4, 149.0, 149.7, 168.7 ppm; MS (MALDI-TOF): m/z: 623 $[Cp^*Co(\eta^5\text{-}\mathbf{1}COMe)]^+$; elemental analysis (%) calcd for $C_{39}H_{36}N_2CoF_6O_2P$ (768.63): C 60.94, H 4.72, N 3.64; found: C 60.91, H 4.72, N 3.61.

[Cp*Co(η^5-1COMe)]BPh$_4$: This compound was obtained in 77 % yield in analogy to the synthesis of the hexafluorophosphate by using a saturated aqueous solution of $NaBPh_4$. It was characterised by X-ray crystallography. Elemental analysis (%) calcd for $C_{63}H_{58}BCoN_2O_2$ (944.91): C 80.08, H 6.19, N 2.96; found: C 79.67, H 6.25, N, 3.21.

[Cp*Co(η^5-1Me$_3$)](CF$_3$SO$_3$)$_3$: Methyl triflate (10 mL) was added dropwise to [Cp*Co(η^4-**1**)] (528 mg, 0.91 mmol). The mixture was stirred for 14 h and subsequently reduced to dryness in vacuo. Ethanol (5 mL) was added to the brownish yellow residue, and the mixture stirred for 10 min. The yellow solid was filtered off, washed with diethyl ether (5 mL) and *n*-hexane (5 mL) and dried in vacuo. Yield 456 mg (47 %). ^{1}H NMR (CD_3CN): δ = 1.69 (s, 15H), 3.62 (s, 6H), 4.10 (s, 3H) 7.32 (m, 4H), 7.54 ("t", 4H), 7.61 (m, 2H), 7.98 (d, J = 8.0 Hz, 2H), 8.12 (m, 2H), 8.62 (d, J = 5.9 Hz, 2H), 8.75 ppm ("t", 2H); ^{13}C{^{1}H} NMR (CD_3CN): δ = 9.7, 47.6, 64.5, 89.2, 93.5, 102.8, 125.3, 127.9, 130.6, 130.7, 131.1, 132.5, 134.0, 144.1, 149.2, 151.6 ppm; MS (MALDI-TOF): m/z: 625 $[Cp^*Co(\eta^5\text{-}\mathbf{1}Me_3)]^+$; elemental analysis (%) calcd for $C_{43}H_{42}N_2CoF_9O_{10}S_3$ (1072.93): C 48.14, H 3.95, N 2.61; found: C 48.17, H 4.24, N 2.91.

General procedure for the preparation of the chelates of 1 with metal dihalides: Equimolar amounts of **1** and the respective metal dihalide MX_2 were stirred in ethanol (10 mL per 100 mg of **1**) at 70 °C for 14 h. The mixture was allowed to cool to room temperature. The solid was filtered off, washed with diethyl ether and *n*-hexane and dried in vacuo. The CO carbon atom gave rise to a low-intensity ^{13}C NMR signal, which sometimes could not be detected with certainty. [(**1**)$ZnCl_2$] was obtained as a red, microcrystalline solid in 72 % yield. ^{1}H NMR ($CDCl_3$): δ = 7.23 (m, 12H), 7.58 (m, 2H), 7.70 (m, 2H), 9.06 ppm (d, J = 5.5 Hz, 2H); ^{13}C{^{1}H} NMR ($CDCl_3$): δ = 125.0, 128.4, 128.6, 129.0, 129.2, 130.3, 130.9, 140.4, 148.7, 149.5, 152.8 ppm; elemental analysis (%) calcd for $C_{27}H_{18}N_2Cl_2OZn$ (522.76): C 62.04, H 3.47, N 5.36; found: C 62.00, H 3.44, N 5.33. [(**1**)Cd(μ-Cl)Cl]$_2$ was obtained in 63 % yield as a violet red, microcrystalline solid. ^{1}H NMR ([D$_6$]acetone): δ = 7.21 (m, 6H), 7.29 (m, 6H), 7.40 ("t", 2H), 7.70 (m, 2H), 8.95 ppm (m, 2H); ^{13}C{^{1}H} NMR ([D$_6$]acetone): δ = 125.5, 127.8, 129.0, 129.4, 130.5, 131.0, 131.2, 140.8, 150.3, 151.4, 154.1 ppm; elemental analysis (%) calcd for $C_{54}H_{36}N_4Cd_2Cl_4O_2$ (1139.54): C 56.92, H 3.18, N 4.92; found: C 56.46, H 3.26, N 4.66. [(**1**)$HgCl_2$] and [(**1**)$HgBr_2$] were obtained as a violet red, microcrystalline solids in 70 % yield. Their NMR spectroscopic data are virtually identical. ^{1}H NMR (CD_2Cl_2): δ = 7.20 (m, 6H), 7.28 (m, 6H), 7.39 (m, 2H), 7.63 (m, 2H), 8.89 ppm (d, J = 4.7 Hz, 2H); ^{13}C{^{1}H} NMR (CD_2Cl_2): δ = 124.7, 126.8, 128.6, 128.8, 129.4, 129.9, 130.3, 139.4, 149.1, 150.5, 153.3, 199.5 ppm. [(**1**)$PdCl_2$] was obtained as a dark red, microcrystalline solid in 48 % yield. ^{1}H NMR (CD_2Cl_2): δ = 7.13 (d, J = 7.8 Hz, 2H), 7.34 (m, 10H), 7.39 (m, 2H), 7.62 (m, 2H), 9.07 ppm (d, J = 5.1 Hz, 2H); ^{13}C{^{1}H} NMR (CD_2Cl_2): δ = 126.6, 127.9, 128.1, 128.7, 128.9, 129.1, 129.8, 140.3, 146.4, 153.3, 153.6, 198.9 ppm; elemental analysis (%) calcd for $C_{27}H_{18}N_2Cl_2OPd$ (563.60): C 57.54, H 3.22, N 4.97; found: C 56.91, H 3.46, N 4.61. [(**1**)$PtCl_2$] was obtained as a brown, microcrystalline solid in 29 % yield. ^{1}H NMR (CD_2Cl_2): δ = 7.11 (d, J = 7.9 Hz, 2H), 7.33 (m, 12H), 7.58 (m, 2H), 9.05 ppm (d, J = 5.6 Hz, 2H); ^{13}C{^{1}H} NMR (CD_2Cl_2): δ = 125.9, 127.1, 128.4, 128.7, 128.8, 129.3, 129.6, 140.0, 147.2, 154.4, 154.5, 199.3 ppm; elemental analysis (%) calcd for $C_{27}H_{18}N_2Cl_2OPt$ (652.31): C 49.72, H 2.78, N 4.29; found: C 48.62, H 2.57, N 3.95.

General procedure for the preparation of the chelates of [Cp*Co(η^4-1)] with metal dichlorides: Equimolar amounts of [Cp*Co(η^4-**1**)] and the respective metal dichloride MCl_2 were stirred in ethanol (10 mL per 100 mg of **1**) at 70 °C for 14 h. The mixture was allowed to cool to room temperature. The solid was filtered off, washed with diethyl ether and *n*-hexane and dried in vacuo. The CO carbon atom gave rise to a low-intensity ^{13}C NMR signal, which could not be detected with certainty. [Cp*Co(η^4-**1**)$ZnCl_2$] was obtained as a dark red, microcrystalline solid in 64 % yield. ^{1}H NMR (CD_2Cl_2): δ = 1.52 (s, 15H), 7.23 (m, 12H), 7.57 (m, 2H), 7.85 (m, 2H), 9.16 ppm (br s, 2H); ^{13}C{^{1}H} NMR (CD_3CN): δ = 9.2, 88.4, 92.0, 97.4, 126.3, 127.7, 129.2, 129.6, 132.6, 133.0, 141.1, 149.7,

151.4 ppm; elemental analysis (%) calcd for $C_{37}H_{33}N_2Cl_2CoOZn$ (716.91): C 61.99, H 4.64, N 3.91; found: C 61.45, H 5.21, N 4.30. [Cp*Co(η^4-**1**)$PdCl_2$] was obtained as a dark red, microcrystalline solid in 67% yield. ^{1}H NMR ([D$_4$]methanol): $\delta = 1.57$ (s, 15H), 7.20 (d, $J = 7.8$ Hz, 2H), 7.27 (m, 4H), 7.35 (m, 6H), 7.59 (m, 2H), 7.93 (m, 2H), 9.07 ppm (d, $J =$ 5.3 Hz, 2H); ^{13}C{^{1}H} NMR ([D$_4$]methanol): $\delta = 7.2$, 84.6, 92.2, 97.4, 123.3, 126.3, 126.4, 129.2, 130.0, 136.1, 152.5, 153.7 ppm; elemental analysis (%) calcd for $C_{37}H_{33}N_2Cl_2OPd$ (757.76): C 58.65, H 4.39, N 3.70; found: C 57.74, H 4.16, N 3.56. [Cp*Co(η^4-**1**)$PtCl_2$] was obtained as a dark brown, microcrystalline solid in 62% yield. ^{1}H NMR (CD_2Cl_2): $\delta = 1.47$ (s, 15H), 7.02 (d, $J = 8.0$ Hz, 2H), 7.27 (m, 10H), 7.40 (m, 2H), 7.68 (m, 2H), 9.14 ppm (d, $J = 5.0$ Hz, 2H); ^{13}C{^{1}H} NMR (CD_2Cl_2): $\delta = 9.2$, 84.1, 85.2, 94.4, 125.8, 128.3, 128.5, 131.1, 131.9, 137.7, 155.4 ppm; no satisfactory elemental analysis could be obtained.

X-ray crystallography: X-ray crystallographic data for **1**, [CpCo(η^4-**1**)], [Cp*Co(η^4-**1**)], [Cp*Co(η^5-**1**COMe)]BPh_4, [Cp*Co(η^5-**1**Me_3)]$(CF_3SO_3)_3$, [(**1**)$PtCl_2$], [(**1**)$ZnCl_2$], [(**1**)$HgCl_2$], [(**1**)$HgBr_2$], [{(**1**)Cd(μ-Cl)Cl_2}] and [Cp*Co(η^4-**1**)$ZnCl_2$] are collected in Table 3. Data collection was performed with a a Siemens $P2_1$ four-circle diffractometer for **1** and [Cp*Co(η^5-**1**COMe)]BPh_4 and with a Nonius Kappa CCD diffractometer for all other compounds. Graphite-monochromatised $Mo_{K\alpha}$ radiation ($\lambda =$ 0.71073 Å) was used in each case. The structures were solved by direct methods. Programs used were Siemens SHELXTL PLUS[25] and SHELXL 97.[26] Full-matrix least-squares refinement on F^2 was carried

Table 3. X-ray crystallographic data.

Compound	**1**	[CpCo(η^4-**1**)]·0.5 $CHCl_3$	[Cp*Co(η^4-**1**)]	[Cp*Co(η^5-**1**COMe)][BPh_4]	[Cp*Co(η^5-**1**Me_3)]$(CF_3SO_3)_3$	[(**1**)$PtCl_2$]·2 CH_2Cl_2
empirical formula	$C_{27}H_{18}N_2O$	$C_{32.5}H_{23.5}Cl_{1.5}CoN_2O$	$C_{37}H_{33}CoN_2O$	$C_{63}H_{58}BCoN_2O_2$	$C_{43}H_{42}CoF_9N_2O_{10}S_3$	$C_{29}H_{22}Cl_6N_2OPt$
formula weight	386.43	570.14	580.58	944.85	1072.90	822.28
crystal system	monoclinic	monoclinic	monoclinic	monoclinic	monoclinic	orthorhombic
space group	$P2_1/c$	$P2_1$	$P2_1/n$	$P2_1/c$	$P2_1/c$	$Pna2_1$
a [Å]	19.021(6)	9.5320(1)	12.5750(1)	17.520(9)	19.2730(2)	20.085(4)
b [Å]	9.188(3)	30.7260(5)	10.8040(1)	14.882(5)	10.7090(1)	11.399(2)
c [Å]	11.532(3)	9.5900(1)	21.2930(3)	20.277(5)	23.9510(3)	26.266(5)
β [°]	99.28(2)	111.8831(8)	95.1240(7)	112.16(5)	114.8440(5)	
V [Å]^3	1989.0(10)	2606.34(6)	2812.57(5)	4896(3)	4485.87(8)	6014(2)
Z	4	4	4	4	4	8
ρ_{calcd} [g cm^{-3}]	1.290	1.453	1.371	1.282	1.589	1.816
μ [mm^{-1}]	0.079	0.842	0.644	0.399	0.620	5.226
F(000)	808	1172	1216	1992	2200	3184
crystal size [mm]	0.5 × 0.4 × 0.3	0.24 × 0.05 × 0.04	0.26 × 0.15 × 0.04	0.3 × 0.2 × 0.1	0.23 × 0.21 × 0.07	0.30 × 0.27 × 0.20
θ range [°]	2.2–30.0	3.0–25.0	3.0–27.5	1.9–22.5	3.0–27.5	2.0–30.0
reflections collected	6053	30621	48577	6533	81348	16869
independent reflections	5782	8980	6428	6282	10249	16869
R_{int}	0.0437	0.067	0.062	0.0773	0.049	
reflections with $I > 2\sigma(I)$	3241	6665	4940	3400	8090	16070
restraints	0	29	0	0	0	1
parameters	271	742	502	430	781	704
GOF on F^2	1.011	1.027	1.041	1.015	1.011	0.992
$R1$[a] ($I > 2\sigma(I)$)/$wR2$[b]	0.0680/0.1490	0.0483/0.1142	0.0391/0.1034	0.0862/0.1961	0.0335/0.0828	0.0251/0.0580
largest diff. peak/hole [e Å^{-3}]	0.315/−0.297	0.527/−0.285	0.542/−0.513	0.565/−0.461	0.495/−0.460	1.450/−1.462

Compound	[(**1**)$ZnCl_2$]·$CHCl_3$	[(**1**)$HgCl_2$]	[(**1**)$HgBr_2$]·0.5 C_3H_6O	[(**1**)Cd(μ-Cl)Cl]$_2$·C_3H_6O	[Cp*Co(η^4-**1**)$ZnCl_2$]·CH_2Cl_2
empirical formula	$C_{28}H_{19}Cl_5N_2OZn$	$C_{27}H_{18}Cl_2HgN_2O$	$C_{28.5}H_{21}Br_2HgN_2O_{1.5}$	$C_{57}H_{42}Cd_2Cl_4N_4O_3$	$C_{38}H_{35}Cl_4CoN_2OZn$
formula weight	642.07	657.92	775.88	1197.55	801.78
crystal system	monoclinic	orthorhombic	orthorhombic	monoclinic	monoclinic
space group	$P2_1/n$	$Pbca$	$Pbcn$	$P2_1/c$	$P2_1/n$
a [Å]	6.8760(1)	13.0660(8)	27.0840(1)	12.0220(2)	9.0860(1)
b [Å]	21.4650(2)	14.8700(8)	13.3410(1)	21.0170(3)	21.9900(3)
c [Å]	18.8700(2)	23.5860(10)	14.5320(2)	20.3800(3)	17.2380(2)
β [°]	96.3740(4)			94.3850(7)	94.6140(5)
V [Å]^3	2767.87(6)	4582.6(4)	5250.81(8)	5134.27(14)	3433.01(7)
Z	4	8	8	4	4
ρ_{calcd} [g cm^{-3}]	1.541	1.907	1.963	1.549	1.551
μ [mm^{-1}]	1.395	6.974	8.933	1.085	1.528
F(000)	1296	2528	2944	2400	1640
crystal size [mm]	0.34 × 0.08 × 0.05	0.16 × 0.14 × 0.09	0.32 × 0.30 × 0.08	0.24 × 0.06 × 0.05	0.30 × 0.06 × 0.06
θ range [°]	2.2–30.0	2.7–30.0	3.0–25.0	3.1–27.5	2.2–30.0
reflections collected	15732	78864	72990	88169	19109
independent reflections	8043	6676	4592	11771	9996
R_{int}	0.0231	0.0786	0.065	0.068	0.0329
reflections with $I > 2\sigma(I)$	6332	5344	4033	8643	7752
restraints	0	0	0	0	0
parameters	334	298	390	783	429
GOF on F^2	1.026	1.083	1.060	1.032	1.020
$R1$[a] ($I > 2\sigma(I)$)/$wR2$[b]	0.0308/0.0743	0.0390/0.0751	0.0297/0.0829	0.0346/0.0833	0.0329/0.0724
largest diff. peak/hole [e Å^{-3}]	0.661/−0.669	1.537/−1.804	2.141/−1.684	1.074/−0.661	0.411/−0.489

[a] $R1 = \Sigma ||F_o| - |F_c|| / \Sigma |F_o|$. [b] $wR2 = \{\Sigma[w(F_o^2 - F_c^2)^2] / \Sigma[w(F_o^2)^2]\}^{0.5}$.

out anisotropically for the non-hydrogen atoms. Hydrogen atoms were included at calculated positions using a riding model, except for the non-disordered hydrogen atoms of [Cp*Co(η^4-**1**)], [Cp*Co(η^5-**1**Me$_3$)](CF$_3$SO$_3$)$_3$, [(**1**)HgBr$_2$] and [(**1**)Cd(μ-Cl)Cl]$_2$, which were refined isotropically. CCDC-238172–CCDC-238182 contain the supplementary crystallographic data for this paper. These data can be obtained free of charge via www.ccdc.cam.uk/conts/retrieving.html (or from the Cambridge Crystallographic Data Centre, 12 Union Road, Cambridge CB2 1EZ, UK; fax: (+44)1223-336-033; or deposit@ccdc.cam.uk).

Acknowledgement

This work was supported by the Fonds der Chemischen Industrie. We thank Prof. Wilhelm Knoche, Dr. Jörg Kleimann and Priv.-Doz. Dr. Rainer Winter for helpful discussions, and Ottilie Thorwarth for electrochemical measurements.

[1] Recent reviews: a) T. Hirao, *Coord. Chem. Rev.* **2002**, *226*, 81–91; b) A. M. Allgeier, C. A. Mirkin, *Angew. Chem.* **1998**, *110*, 936–952; *Angew. Chem. Int. Ed.* **1998**, *37*, 894–908.

[2] Recent reviews: a) A. E. Kaifer, M. Gómez-Kaifer, *Supramolecular Electrochemistry*, Wiley-VCH, Weinheim, **1999**, Chap. 10; b) A. E. Kaifer, S. Mendoza in *Comprehensive Supramolecular Chemistry*, *Vol. 1* (Ed.: G. W. Gokel), Pergamon, Oxford, **1996**, Chap. 19.

[3] Selected reviews: a) I. Haiduc, F. T. Edelmann, *Supramolecular Organometallic Chemistry*, Wiley-VCH, Weinheim, **1999**, Chap. 2.1.5; b) P. D. Beer, *Adv. Inorg. Chem.* **1992**, *39*, 79–157; c) P. D. Beer, *Chem. Soc. Rev.* **1989**, *18*, 409–450.

[4] See, for example, a) A. Gouloumis, R. C. Lawson, P. Vázquez, L. Echegoyen, T. Torres, *Tetrahedron* **2002**, *58*, 961–966; b) M. Gómez-Kaifer, P. A. Reddy, C. D. Gutsche, L. Echegoyen, *J. Am. Chem. Soc.* **1994**, *116*, 3580–3587.

[5] B. Eistert, G. Fink, M. A. El-Chahawi, *Liebigs Ann. Chem.* **1967**, *703*, 104–108.

[6] H. van Willigen, W. E. Geiger, Jr., M. D. Rausch, *Inorg. Chem.* **1977**, *16*, 581–584.

[7] See, for example, a) R. Gleiter, R. Roers, F. Rominger, B. Nuber, I. Hyla-Kryspin, *J. Organomet. Chem.* **2000**, *610*, 80–87; b) J. W. Chinn, Jr., M. B. Hall, *Organometallics* **1984**, *3*, 284–288; c) R. Hoffmann, P. Hoffmann, *J. Am. Chem. Soc.* **1976**, *98*, 598–604.

[8] This effect has long been known. See, for example: E. Weiss, W. Hübel, *J. Inorg. Nucl. Chem.* **1959**, *11*, 42–55.

[9] T.-L. Ho, *Chem. Rev.* **1975**, *75*, 1–20.

[10] P. Jutzi, U. Siemeling, A. Müller, H. Bögge, *Organometallics* **1989**, *8*, 1744–1750.

[11] W. L. Steffen, G. J. Palenik, *Acta Crystallogr. Sect. B* **1976**, *32*, 298–300.

[12] K. Satoh, T. Suzuki, K. Sawada, *Monatsh. Chem.* **2001**, *132*, 1145–1155.

[13] A. J. Canty, C. L. Raston, B. W. Skelton, A. H. White, *J. Chem. Soc. Dalton Trans.* **1982**, 15–18.

[14] C. J. Matthews, W. Clegg, S. L. Heath, N. C. Martin, M. N. Stuart Hill, J. C. Lockhart, *Inorg. Chem.* **1998**, *37*, 199–207.

[15] a) D. M. P. Mingos, *Essential Trends in Inorganic Chemistry*, Oxford University Press, Oxford, **1998**, Chaps. 3.5, 5.5; b) J. Huheey, E. Keiter, R. Keiter, *Anorganische Chemie*, 2nd ed., de Gruyter, Berlin, **1995**, Chap. 4.

[16] J. A. Tossell, D. J. Vaughan, *Inorg. Chem.* **1981**, *20*, 3333–3340.

[17] P. Colamarino, P. L. Orioli, *J. Chem. Soc. Dalton Trans.* **1975**, 1656–1659.

[18] All potentials are referred to the ferrocenium/ferrocene couple, whose formal electrode potential versus SCE is 0.46 V in dichloromethane and 0.40 V in acetonitrile (0.1 M [NBu$_4$]PF$_6$ supporting electrolyte); see N. G. Connelly, W. E. Geiger, *Chem. Rev.* **1996**, *96*, 877–910.

[19] *CRC Handbook of Chemistry and Physics*, 82nd ed. (Ed.: D. R. Lide), CRC Press, Boca Raton, FL, **2001**, Table 8-127.

[20] W. Ried, A. Göbel, *Chem. Ber.* **1967**, *100*, 3405–3412.

[21] P. Bergmann, H. Paul, *Chem. Ber.* **1967**, *100*, 828–835.

[22] S. A. Frith, J. L. Spencer, *Inorg. Synth.* **1985**, *23*, 15–21.

[23] U. Siemeling, B. Neumann, H.-G. Stammler, O. Kuhnert, *Polyhedron* **1999**, *18*, 1815–1819.

[24] R. P. Hughes, A. S. Kowalski, J. R. Lomprey, D. R. Neithamer, *J. Org. Chem.* **1996**, *61*, 401–404.

[25] G. M. Sheldrick, SHELXTL PLUS, Siemens Analytical Instruments, Madison, WI, **1990**.

[26] G. M. Sheldrick, SHELXL 97, University of Göttingen, Göttingen, **1997**.

Received: May 12, 2004
Published online: October 7, 2004

